Results in Engineering 6 (2020) 100118

Contents lists available at ScienceDirect

Results in Engineering

journal homepage: www.editorialmanager.com/rineng/Default.aspx

Performance investigation of high-proportion Saudi-fly-ash-based concrete

Y.H. Mugahed Amran [a,b,*], Mariantonieta Gutierrez Soto [c], Rayed Alyousef [a], Mohamed El-Zeadani [d], Hisham Alabduljabbar [a], Vegard Aune [e,f]

[a] Department of Civil Engineering, College of Engineering, Prince Sattam Bin Abdulaziz University, 11942, Alkharj, Saudi Arabia
[b] Department of Civil Engineering, Faculty of Engineering and IT, Amran University, 9677, Quhal, Amran, Yemen
[c] Department of Civil Engineering, University of Kentucky, 161 Raymond Building, Lexington, KY, 40506, USA
[d] Department of Civil Engineering, Faculty of Engineering, Universiti Putra Malaysia, 43400, Serdang, Selangor, Malaysia
[e] Structural Impact Laboratory (SIMLab), Department of Structural Engineering, NTNU, Norwegian University of Science and Technology, Trondheim, Norway
[f] Centre for Advanced Structural Analysis (CASA), NTNU, Trondheim, Norway

ARTICLE INFO

Keywords:
Saudi-fly-ash (SFA)
Fresh and hardened properties of SFA
Microstructure of SFA-Based concrete
Thermal profile

ABSTRACT

Approximately 544 million tonnes of fly ash (FA) are generated annually worldwide, 80% of which is disposed of in landfills. Thus, using FA as a replacement for cement has turned out to be popular in construction industries around the world because of its strong properties and crucial role in decreasing the volume of pollutants and CO_2 produced by cement production. Meanwhile, the use of Saudi FA (SFA) as a suitable supplemental cementing material to partly substitute cement in the design of SFA-based concrete is highly imperative. An extensive experimental study was conducted to utilize increased levels of SFA in the production of concrete. Six concrete mixes were utilized: five out of the six mixes were made with different levels of SFA and one mix was used as a reference. This study presents the findings of using different volumes of SFA with variable proportions (i.e., 0%, 10%, 20%, 30%, 40%, and 50%). Experimental tests were performed to study the properties of SFA-based concrete, including slump test, air content, setting times, thermal profile, specific gravity, sieve gradation, flexural strength, compressive strength, tensile strength, wear depth, resistance to abrasion, and elasticity modulus, at different time intervals for one year. However, the hardened strength properties and resistance to abrasion exhibited incessant and substantial enhancement at 56 days and up to one year, which is generally attributable to the pozzolanic reaction of SFA. Subsequently, all strengths increased when thermal heat decreased, and test results indicate that SFA can potentially substitute cement in concrete by up to 50% for the fabrication of structural concrete elements in the construction industry.

1. Introduction

Concrete is the second most used construction material after water, with an annual global consumption rate of approximately 25×10^9 metric tonnes; and the annual cement used is nearly 3.3 billion tonnes [1]. Concrete is widely used because of its excellent durability, low cost, availability of raw materials, and ability to be fabricated into any shape [2,3]. The binding methods and materials utilized for making concrete are also vital in construction technology [4], and thus far, cement is the most widely used binding material in concrete and RC applications [2]. The worldwide manufacturing of cement increases by 9% annually and generates almost 1 tonne of CO_2 gas [5]. Both China and India are the largest coal consumers in 2018 with a consumption rate of 1906.7 and 452.2 million metric tonnes of oil equivalent, respectively, as shown in Fig. 1 [6]. In particular, cement production emits approximately 1.5 billion tonnes of CO_2 yearly or 9% of the total emissions contributed by multiple sectors worldwide [5,7,8]. The top 10 CO_2 polluting countries, thanks to cement manufacturing, are presented in Fig. 2. The greenhouse influence avoids the reflection of solar radiation back into atmosphere, thus preserving the regular heat on the surface of the Earth between 15 °C and 18 °C [9]. The CO_2 concentration in the air has lately augmented by 30% or approximately 467 million tonnes (Mt), 83% of which comes from the UK [9–13]. Therefore, an alternative sustainable supplemental cementing material (SCM) with similar or improved properties is required [14]. Considerable effort has been exerted recently to enhance the production of sustainable construction materials. Among such efforts is the replacement of hydrated lime in mortars with kaolinitic clay [15]. Hydrated lime in mortars is particularly important as it ensures sufficient

* Corresponding author. Department of Civil Engineering, College of Engineering, Prince Sattam Bin Abdulaziz University, 11942, Alkharj, Saudi Arabia.
E-mail addresses: m.amran@psau.edu.sa, mugahed_amran@hotmail.com (Y.H. Mugahed Amran).

https://doi.org/10.1016/j.rineng.2020.100118
Received 1 February 2020; Received in revised form 21 March 2020; Accepted 21 March 2020

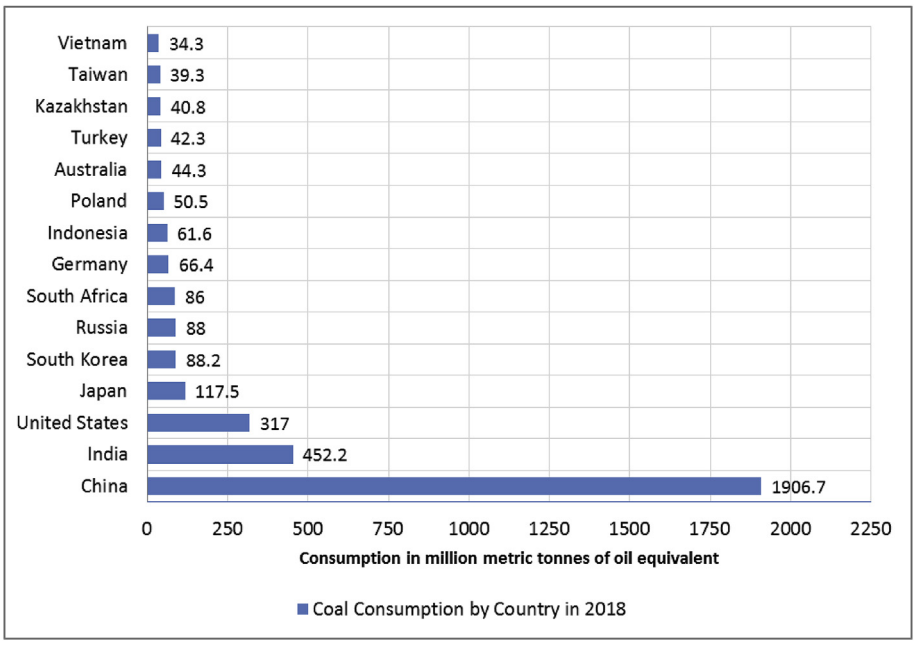

Fig. 1. Countries with the largest coal consumption worldwide in 2018 [6].

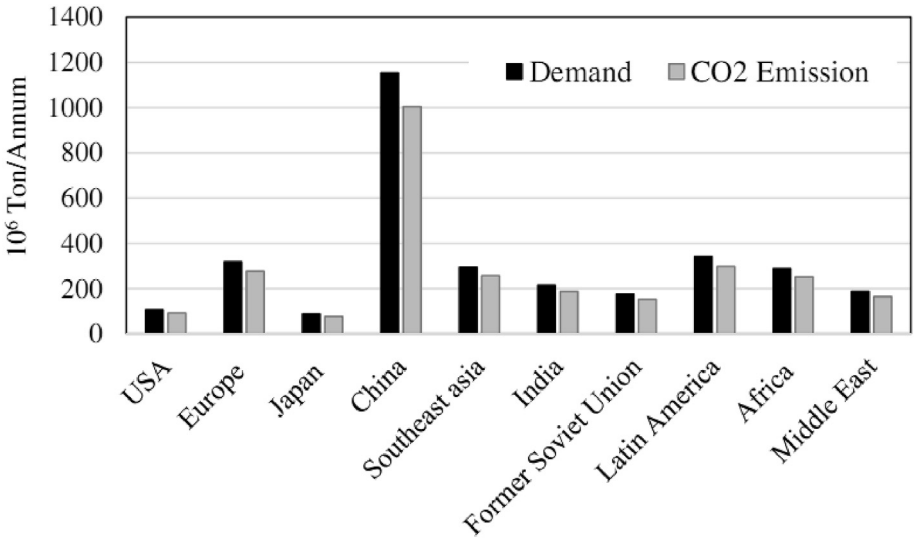

Fig. 2. Estimated demand for cement and CO_2 emission by 2020 [32].

workability. Typical mortar compositions have traces of cement: hydrated lime: sand that vary from 1:1:6 to 1:2:9. That is, hydrated lime is generally equal to or double the amount of cement in mortars [16]. This is alarming as the cost of hydrated lime could be 10–15% greater than cement [17]. Furthermore, the production of 1 tonne of hydrated lime could result in emitting 1.2 tonnes of CO_2 into the atmosphere; thereby exacerbating the environmental problem [18]. As an alternative, researchers have attempted to use kaolinitic clay as a suitable replacement for hydrated lime [15] and results have shown that with up to 50% hydrated lime replacement, the fresh and mechanical properties of the mortars were perfectly adequate. Besides the incorporation of kaolinitic clay in mortars, and in an attempt to promote sustainable practices in construction, several researchers have investigated the reuse of solid wastes, such as stone residues, in coating mortars for building construction [19,20]. For instance, the processing of stones, such as granite, results in huge amount of residues, and up to 80% of loss occurs from the original rocks [19]. As such, studies on the incorporation of granite residue as a replacement for sand in mortars have shown positive results with a replacement level of up to 40% [19,21]. In addition, researchers have also attempted to enhance the production of sustainable cement and the performance of geopolymer cement/concrete (GeoPC) [14,22,23]. This by-product is called fly ash (FA) or pulverized fuel ash in the UK [24]. FA is a coal incineration application that comprises fine particles of fuel obtained from coal-fired boilers and flue gases, and is used as SCM, thereby reducing the utilization of cement in concrete and decreasing the CO_2 emissions and energy exhaustion [25,26]. Approximately 544 Mt of FA are generated annually worldwide, 80% of which are disposed of in landfills [27]. A simplified schematic diagram of FA formation during pulverized fuel combustion is depicted in Fig. 3. In 1949, Australia recorded the first FA application in construction, having less than 7% lime [28]. While in the United States (US), FA was introduced from Chicago [29], and subsequently became popular in the US in the 1930s after publishing the findings of a study on concrete encompassing FA [30]. The properties of FAs differ depending on the hopper from where

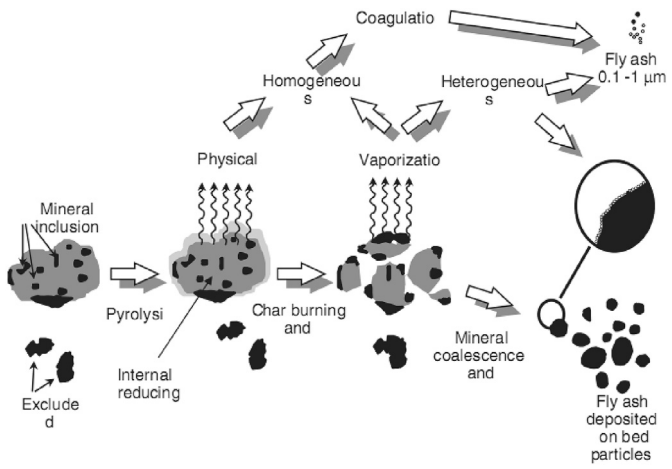

Fig. 3. Schematic of the formation of FA during coal combustion [33].

they are composed. Stakeholder interviews have indicated that the prices of FA have increased between 85% and 100% in 2012–2016 owing to low FA availability [31].

However, over 6×10^7 tonnes and 11.2×10^7 tonnes of FA are annually produced in the US and India (occupying 26,304 ha in India), respectively, by burning coal for electric power production [34,35]. The majority of FAs are disposed of as solid wastes in landfills or surface impoundments, thereby resulting in a serious problem of inadequate disposal. Attempts to recycle wastes are partially successful in reducing 43% of the total wastes [36,37]. Under such a condition, generating FA remains important and its financial and green application technology is desired [38–40]. For instance, FA has been used to form cementitious matrices together with natural fibre reinforced (NER) cementitious composites that incorporate 20–30 mm strands of resin coated and uncoated flax/wool twine in an effort to reduce the use of ordinary Portland cement (OPC) and also to reduce the use of synthetic fibres [41]. The study illustrated that the use of flax/wool twine enhanced the performance of the mortars as opposed to the unreinforced and uncoated samples. Such new applications are explored in sound and thermal insulation applications in buildings, and the goal is to achieve energy efficiency. By doing so, heating costs, energy demands and environmental impacts will diminish. Advances in concrete technology have also included the use of silica-based crystallizing impregnant [42] and sodium acetate [43] to enhance the performance of concrete mixes. Furthermore, numerous studies in different countries, including Saudi Arabia, have assessed the potential of mixing various wastes with FA as raw materials [1,14,36,37,44–55]. FA is frequently utilized as a pozzolan to make plaster and a partial or full substitution for cement in the manufacturing of concrete [38]. Pozzolans guarantee plaster setting and afford concrete with further protection from chemical attacks and wet environments [56]. The selection of materials to make GeoPC relies on factors such as disposal urgency, availability, difficulty of recycling, and final use [57]. Published studies have indicated FA's favorable potential for producing different types of concrete for several applications. FA, along with other pozzolans, is extensively approved for current use as a SCM constituent in concrete by main codes, with nearly 55% of FA content in the pozzolanic CEM IV in BS EN 197–1 [58]. This can be attributed to the fact that FA is recognized as an eco-friendly material as its consumption aids in reducing the carbon footmark of cement manufacturing, which is nearly 5% of the overall CO_2 emissions worldwide. However, the application of FA in high-performance and self-consolidating concrete remains limited, particularly in Saudi Arabia, and research on the usage of Saudi FA (SFA) as a potential SCM for the partial replacement of cement content is crucial. Construction industries in several countries demand the increased production of SCMs, such as FA, given their indispensable role in reducing the amount of pollutants and CO_2 generated by cement production. Many investigators have attempted to lower the use of cement by producing eco-friendly concretes that use certain byproduct materials. The current study aims to investigate the performance properties of SFA as a partial cement substitution for producing SFA-based concrete with the optimum dosage of superplasticizers (SPs) at different proportions of SFA (i.e., 0%, 10%, 20%, 30%, 40%, and 50%), including air content, slump test, unit weight, setting times, thermal and microstructure profiles, specific gravity, sieve gradation, compressive strenght, tensile strength, flexural strength, wear depth, resistance to abrasion, and modulus of elasticity.

2. Experimental work

The experimental program for this study involved six different concrete mixes. The percentages of SFA content in the concrete mixes were set at 0%, 10%, 20%, 30%, 40%, and 50%, by weight of cement. One mix (i.e., 0% SFA) was set as the reference. In general, geopolymer-FA-based concrete, which is made by the polymeric reaction of alkaline liquid with the entire substitution of cement by FA (e.g., SFA), has numerous limitations, such as the need for heat curing and deferral in the setting times. Both thermal profile and setting time tests were conducted. Furthermore, primal tests, which are tests on the physical and chemical properties of the related materials, were performed. The preparation, mixing, fabrication, curing, and testing procedures are presented in detail in the following subsections.

2.1. Properties of cement and SFA

Cement functions as a binder material that sets, stabilizes, and could interact with SCMs. Saudi ordinary Portland cement (OPC) Type I with high C_3S was used (see Table 1). OPC cement Type I satisfies the requirements of ASTM C 150 [59]. Table 1 shows the primal test results, and SFA with 2.51 specific gravity was utilized in the design mix investigated in this study. The chemical and physical properties of SFA were examined (see Table 2) in line with ASTM C 150 [59] and ASTM C 311 [60]. The fineness of SFA was 365.2 m^2/kg, as presented in Table 2. However, the replacement of OPC was measured by weight, yielding a high amount of SFA in the mixes as the specific gravity of SFA is lower than that of the cement. When high fine particles are found in the system, the SFA particles do not react but continue to assist as the nuclei for the

Table 1
Cement physical and chemical properties.

Saudi cement Type I with high C_3S			
Properties		Tests values	Requirement: ASTM C 150 [59]
SO_3, %		3.14	3.0 max
CaO, %		63.71	44.4 min
MgO, %		1.21	6.0 max
SiO_2, %		21.21	33.1 max
Al_2O_3, %		5	6.0 max
Fe_2O_3, %		3.78	6.0 max
Loss on ignition (LOI), %		1.52	–
Element Iridium (IR), %		0.44	–
Fineness (retained on 90-μm sieve), %		7.5	10 max
Fineness: specific surface (air permeability test) (m^2/kg)		272	225 min
Standard/normal consistency, %		30	–
Vicat time of setting (min): (Initial)		111	30 min
Vicat time of setting (mn): (Final)		191	600 max
Compressive strength (MPa)	3 days	24.2	22.0 min
	7 days	35.7	31.5 min
	28 days	47.7	43.0 min
	56 days	57.3	55.0 min
Specific gravity		3.19	–

Table 2
SFA physical and chemical properties.

Parameters, (%)	Recorded Values	Requirement ASTM C 618 (%) [63]
SiO_2, (%)	53.8	–
Moisture, (%)	0.3	3.0 max
Fe_2O_3, (%)	5.2	–
$SiO_2 + Al_2O_3 + Fe_2O_3$, (%)	84.8	70.0 min
Al_2O_3, (%)	26.72	–
Na_2O, (%)	0.6	1.5 max
CaO, (%)	5.7	–
SO_3, (%)	1.5	5.0 max
TiO_2, (%)	1.4	–
MgO, (%)	2.3	5.0 max
K_2O, (%)	0.7	–
LOI (1000° C)	1.85	6.0 max
Fineness (m^2/kg)	365.2	–
Specific gravity	2.51	–
Plasticity	Non plastic	–
Optimum moisture content (%)	37.0–19.0	–
Maximum dry density (gm/cc)	0.9–1.58	–
Coefficient of consolidation C_v (cm^2/sec)	$1.70 \times 10^{-5} - 2.03 \times 10^{-3}$	–
Angle of internal friction (j)	300–400	–
Cohesion (kN/m^2)	Negligible	–
Permeability (cm/sec)	$8 \times 10^{-6} - 7 \times 10^{-4}$	–
Compression index C_c	0.05–0.4	–
Coefficient of uniformity	3.3–10.9	–

Table 3
Aggregates physical properties.

Property	Average values	
	Fine aggregate,	Coarse aggregate
Type of sand	Nature sand	River stones
Specific gravity	2.62	2.60
Maximum size (mm)	4.75	12.5
SSD absorption (%)	0.88	1.14
Fineness modulus	2.24	5.94
Unit weight (kg/m^3)	1703	1687
Void (%)	33.3	37.8

development and promotion of the hydration of cement outputs.

2.2. Properties of aggregates

In this study, both aggregates (coarse and fine) were verified in accordance with ASTM C 136 [61]. The fine aggregates were river sand with a maximum size of 4.75 mm (see Table 6) and specific gravity of 2.62 (see Table 3). Meanwhile, the coarse aggregates were crushed river stones with a maximum size of 12.5 mm (see Table 6) and specific gravity of 2.60 (see Table 3). Tables 3 and 6 show the physical properties and sieve analysis, respectively, of both aggregate types.

2.3. Superplasticizers

This study used polycarboxylate ether (PCE) as a suitable SP to enrich the workability of fresh SFA-based concrete. The integration of SFA can increase the complexity of the harmonization relationship between SCMs and SP. Hence, a basic concern on the choice of well-suited interrelating pair emerges. This study showed that the best SP is detached directly from the pore solution after mixing. The assimilation volume of the blend is principally measured using the cement type, fineness, and molecular weight. The SP assimilation relies on the volume of C_3S and presence of the sulphates of soluble alkali in the blend paste. The current study illustrated that the integration of SFA in concrete lowers the need for SP (PCE) to gain the same slump flow because the concrete merely encompasses cement as binder. The properties of PCE as a suitable SP was investigated through experiments consistent with ASTM C 494 [62] (see Table 4).

Table 4
Properties of SPs.

Type of Superplasticizer	PCE
Relative density at 25 °C	1.08
Dry material content (%)	33.72
pH value	7.2
Chloride ion content (%)	0.008

Table 5
SFA-based concrete mixture proportions.

No. of Batch (Mixture)		B00	B10	B20	B30	B40	B50
FA	%	0	10	20	30	40	50
FA	kg/m^3	0	280	240	160	180	200
Cement, C		400	280	260	240	220	200
Water, W		160	160	160	160	160	160
Superplasticizer	l/m^3	2.2	2.3	2.4	2.5	2.6	2.7
W/(C + FA)	–	0.41	0.41	0.41	0.40	0.41	0.40
Air temperature	◦C	29	28	27	26	25	25
Air content	%	3.3	3.4	3.5	3.6	3.7	3.8
Concrete temperature	◦C	29	29	26	25	25	25
Slump	mm	60	70	75	80	100	110
Coarse aggregate	kg/m^3	1275	1135	1135	1126	1130	1132
Fine aggregate		620	620	620	619	616	621
Concrete density		2456	2429	2416	2305	2306	2313

2.4. Proportions of mixture

In the experimental work, six mixtures were prepared and designed in consistence with ASTM C 618 [63] to have a strength of 45.52 MPa on the 28th day. One reference mixture and five other concrete mixtures were fabricated by substituting OPC with 0%, 10%, 20%, 30%, 40%, and 50% SFA (Class C ash) by mass and labelled as B00 (reference mixture), B10, B20, B30, B40, and B50, respectively (see Table 5). The water/SCM ratio was maintained to study the influences of substituting OPC with a high amount of SFA when other related parameters were nearly maintained to achieve the desired compressive strength with structural grades for all the SFA proportions.

2.5. Primary tests

2.5.1. Sieve analysis of the aggregates

The sieve test analysis was performed on coarse aggregates (see Table 6) using a sufficient amount of aggregate according to ASTM C 136; coarse aggregates were placed over a number of sieves to obtain the size of the aggregates (i.e., grading analysis) on the basis of the sieve openings. After the sieve analysis test, the percentage of passing (i.e., fineness) was weighed and the cumulative weights were calculated accordingly and articulated as a level of the entire weight. A known weight sample of fine aggregate (i.e., fine sand; see Fig. 4 and Table 6) was dried by placing the sample in an oven at 110 ± 5 °C. The sample was removed from the oven and weighed thereafter. The aggregate exhibited at least 95% passing through sieve no. 8 and 85% passing through sieve no. 4. At least 5% remained on sieve no. 8. Thereafter, a nest of sieves were placed in a descending order and the sample was poured onto the top sieve and shaken using a mechanical shaker. After the test, each sieve was weighed as the weight of retained aggregate and the passing percentage was also computed. The combination of aggregates with the grading requirements was consistent with BS 882:92 (see Table 6 and Fig. 4) [57].

2.5.2. Setting times of cement

A Louis Vicat plunger was utilized to measure the normal consistency

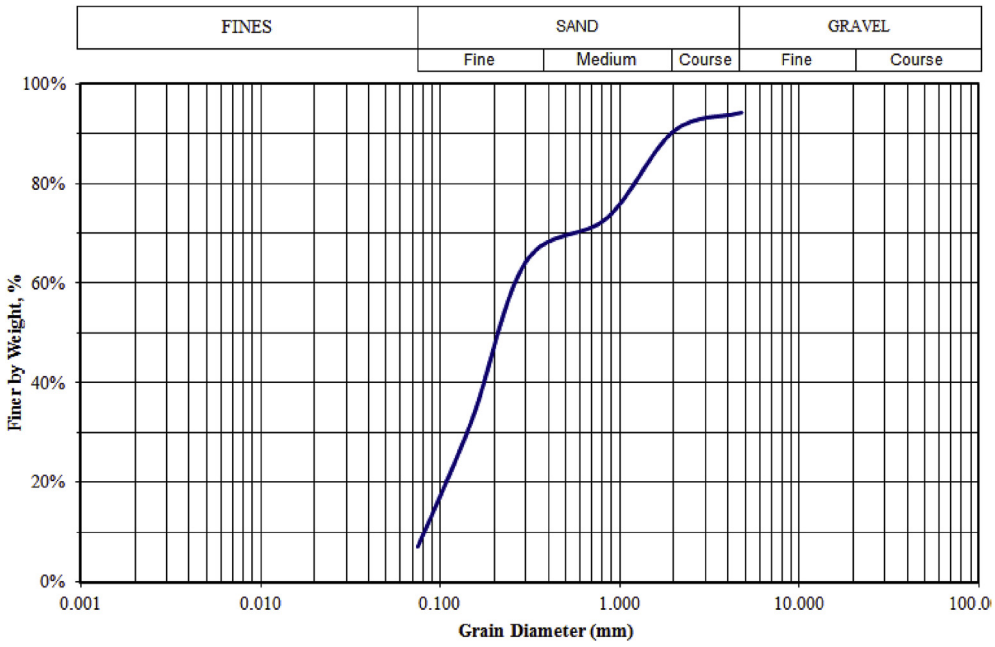

Fig. 4. Grain size analysis of a fine aggregates sample.

Table 6
Sieve analysis of the aggregates.

Fine aggregates			Coarse aggregates		
Sieve no.	Percent passing	Requirement: BS 882:92 [64]	Sieve size	Percent passing	Requirement: BS 882:92 [64]
4.75 mm	94.2	90–100	14 mm	100	100
2.36 mm	90.5	85–100	12.5 mm	92	95–100
1.18 mm	73.1	75–100	9.5 mm	69	40–85
600 μm	64.3	60–79	4.75 mm	9	0–10
300 μm	32.5	12–40	–	–	–
150 μm	7.1	0–10	–	–	–

of cement with interpolation to determine the amount of water needed for the initial setting time (IST). In general, setting denotes the alteration in consistency of a mixture from a liquid to a stiff state that results from the hydration of cementing mixtures. Therefore, setting was controlled by the chemical reactions that occurred immediately after the water, SFA, and cement were mixed together. The final and initial setting times of the concrete set were measured by the procedure of penetration resistance in line with ASTM C 403 [65]. At the fresh state, the test included the elimination of coarse aggregates by sieving through seive no. 4 (4.75 mm). Before starting the experiment, a normal consistency test was performed using the Vicat apparatus with a plunger to achieve penetration for approximately 111 min; and the load needed to initiate the 10 ± 1-mm penetration depth of the indicator was divided by the bearing surface area of the indicator. The paste reaches a penetration resistance of above 3.5 MPa, called the IST, when the required intial contact of water and cement is achieved (see Table 1). IST must be performed to give the paste normal consistency. The materials of the reference sample batch were prepared using 1000 g of OPC. For the other sample batches, the cement was partly substituted with SFA at different proportions to attain a penetration of 25 ± 1 mm. The final setting time (FST) was achieved when the depth of penetration resistance exceeded 25 MPa. Table 1 and Fig. 7 present the test data of both the final and initial setting times.

Table 7
Specific gravity of SFA.

Property	Data
Average bulk dry	2.41
Average bulk SSD	2.47
Average apparent	2.51
Average absorption	1.93%

2.5.3. Specific gravity

To measure the specific gravity of the coarse and fine aggregates used, the process started by weighing a sample of 4500 g from the used aggregates in accordance with ASTM C 127 [66] through a 4.75-mm sieve. This procedure was meant to determine the coarse aggregates volume and retained sample on the sieve used. Furthermore, the entire absorption of the aggregates was limited to 1.93%, which is below 2%, thereby considerably matching the requirement of the design standard. Meanwhile, the specific gravities of the used SFA and cement were 2.51 (see Table 7) and 3.19, respectively. In the case of the mixtures encompassing SFAs where the f_{fw} fraction of the cement is substituted with a similar SFA weight, fractions of cement, SFA, and water could be reported as given by Equation (1). In the equation, ρ_f and v_f are the specific gravity and fraction of SFA, respectively. This was computed as 1.80 by considering the specific gravity of C–S–H obtained from the pozzolanic reaction. However, the efficient volume of SFA was subsequently identified to be 2.14. Bulk specific gravity was computed using the proportion of the weight of the given aggregate volume to an equal volume of water as follows (Equation (2)):

$$v_f = \frac{\frac{f f_w}{\rho_w}}{w_c + \frac{1-f f_w}{\rho_w} + \frac{f f_w}{\rho_f}} \quad (1)$$

$$G_{sb} = \frac{mass\ oven\ dry}{SSD - mass\ saturated\ sample} \quad (2)$$

- Bulk volume = solid volume + water pore volume

Fig. 5. Slump test of 20% SFA-based concrete as an example.

$$\text{In addition, apparent } G_{sa} = \frac{mass\ oven\ dry}{mass\ oven\ dry - mass\ saturated\ sample} \quad (3)$$

The bulk saturated-surface dry (SSD) specific gravity can also be obtained by the ratio of SSD to the weight volume of water using Equation (4):

$$\text{specific gravity SSD} = \frac{SSD}{SSD\ -\ mass\ saturated\ sample} \quad (4)$$

2.6. Preparation, fabrication, casting and remedy of test specimens

The coarse and fine aggregates were made ready under the SSD condition beforehand adding them into the concrete mixture. The alkaline activator was also arranged in the workroom by fraternization sodium hydroxide and sodium silicate solutions at the appropriate proportion approximately half an hour prior to the real mixing of the SFA-based concrete. The SFA and aggregates were initially dried and assorted in a concrete blender. Thereafter, activator solutions were added and continuously mixed for another 5 min to make fresh SFA-based concrete. SP and water were subsequently added during the addition of the last five mixtures (i.e., B10 to B50). A total of 864 samples were prepared, mixed and cast in ready-steel molds in line with ASTM C 31 [67], and the samples were equally divided as follows; 150 mm × 300 mm cylinder samples (a total of 216 samples), 150 mm cubic samples (a total of 216 samples), 65 mm × 65 mm × 60 mm samples (a total of 216 samples), and 105 mm × 105 mm × 515 mm prism samples (a total of 216 samples). After casting, all samples were enclosed with hessian and plastic canvas and left at ambient temperature of approximately 24 °C and 70 ± 10% relative humidity for 24 h. All samples were de-molded after 1 day and submerged in a water tank for curing under ambient conditions until the stipulated time of testing. The prepared samples were used to test for the splitting tensile strength (STS), compressive strength, abrasion resistance, flexural strength, and elasticity modulus.

2.7. Fresh and hardened concrete properties

2.7.1. Fresh tests

All fresh concrete properties, such as air content, slump test, workability (BS EN 12350: Part 2) [68], and unit weight, were measured according to ASTM C 143 [69]. The actual test procedure is presented in Fig. 5 and Table 5 tabulates the reported results.

2.7.2. Hardened tests

To obtain the hardened strengths of the concrete, the compressive, flexural and splitting tensile strengths, and elasticity modulus tests were performed at 3, 14, 28, 56, and 91 days and one year from the casting date. The tests were performed in line with the ASTM C 39 [70], ASTM C 496 [71], ASTM C 78 [72], and ASTM C 469 [73], respectively. The depth of wear and abrasion resistance were also measured in accordance with ASTM C 779 [74]. All samples were completely dried out of water prior to testing to read and record the test results properly and with minimal errors. The findings indicate that the results were influenced by the wet-mixing time, curing time, curing temperature, particles size (fineness of SFA), type, and source of the aggregates and the testing condition [3,59].

2.7.3. Thermal profile

The measurement of the thermal profile is commonly conducted during the test, thereby determining the temperature of the sample until 7 days from the time of casting. This procedure facilitates the elucidation of the influences of SFA with respect to the temperature of the sample. The test was performed by connecting the test samples to a device using wire, which was calibrated to record the temperature. The temperature at the center of the samples (two samples for each group) was monitored. Fig. 6 shows the average temperature change against time. The temperature rate of the SFA-based concrete mortars increased slightly in comparison with the reference mortar. However, the peak temperatures were nearly 31.5 °C, 29.7 °C, 28.9 °C, 28.4 °C, 27.5 °C, and 27.1 °C for mortars B00, B10, B20, B30, B40, and B50, respectively. When the SFA level of replacement increased, the temperature peak was marginally delayed

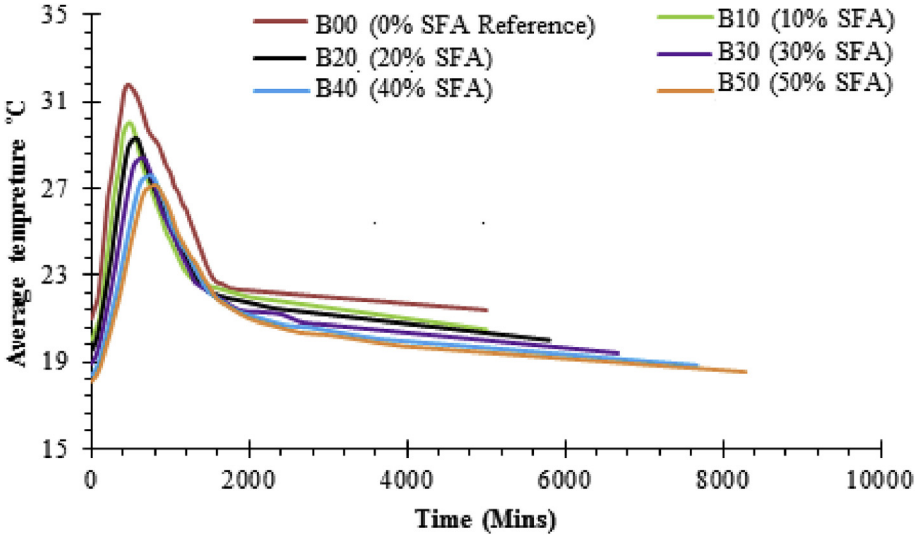

Fig. 6. Average temperature profile vs. time of testing.

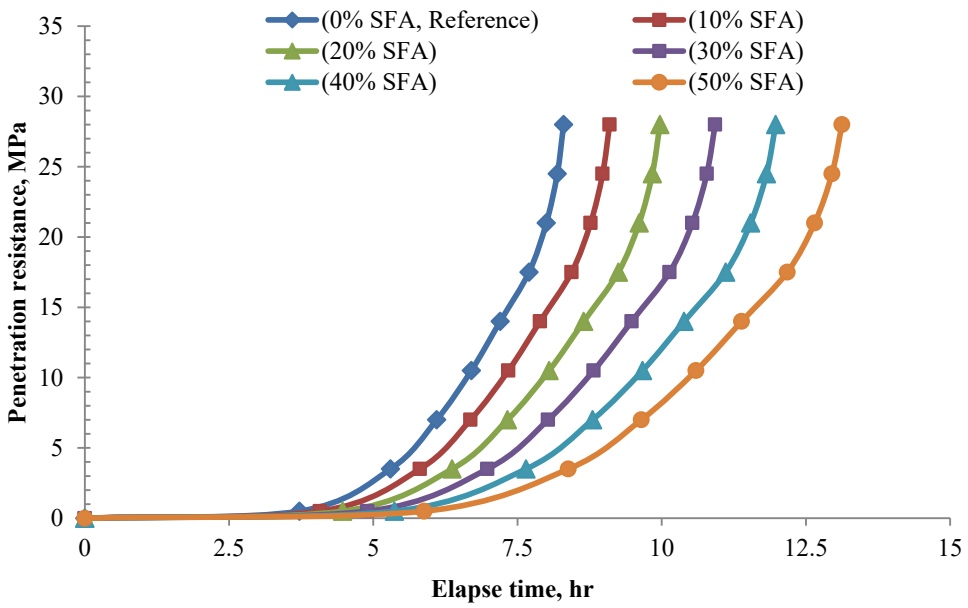

Fig. 7. Penetration resistance vs. elapse time.

and subsequently decreased.

2.7.4. Microstructure profile

A scanning electron microscope (SEM) is a visual device utilized to magnify concrete cracks and fractures or analyze the materials that are not distinguishable using an optical microscope. SEM is considered an innovative method to comprehend the influence of SFA on the morphology of the paste. In the X-ray diffraction (XRD), the XRD device shoots X-rays that assist with the identification of minerals and other crystalline materials. XRD is also beneficial for determining fine-grained materials, such as SFA or cement. XRD is a significant method for quantitatively and qualitatively analyzing cement pastes and cement. However, a SEM prepared with an energy dispersive X-ray analyzers (SEM- EDX) is a significant complement to a visual microscope when inspecting novel, old, and worn concrete. SEM was used to obtain images from full-sized concrete samples. Thereafter, these images were employed to investigate the generation and contact of compressive stress-induced microcracks and the influence of detention on the microcrack performance. XRD analysis was performed at room temperature via powder XRD with a filtered 0.154-nm C_u, Kα radiation. The SFA samples were skimmed in an incessant mode from 100 °C-800 °C with a scanning rate of approximately 20 per min.

3. Analysis and discussion of results

The experimental test results were analyzed and discussed in the contexts of air content; slump test; unit weight; setting times; thermal and microstructure profiles; specific gravity; sieve gradation; compressive, tensile, and flexural strengths; wear depth; resistance to abrasion; and modulus of elasticity.

3.1. Setting times

The effect of SFA on setting time may be in the physical and chemical properties [1,11–13]. Physically, utilizing SFA to replace an amount of OPC entails that the greater the OPC volume in the mixture, the higher the OPC setting will be, thereby accelerating the hydration of cement outputs. Chemically, SFA could influence cement hydration and some SFAs can also react themselves. Fig. 7 shows the penetration resistance versus the elapsed time for concrete containing different levels of SFA. The setting times of the reference samples were delayed longer than those of the SFA-based concrete mortars, depending on the level of SFA content addition and the reduction of cement content in the concrete mortars. However, the increase in SFA volume without any alteration in cement content can delay the setting of SFA-based concrete mortars even further. This result is evident from those of previous studies [58]. That is, the longer deferral in setting time of SFA (Class C FA) than that of Class F FA could be accredited to the higher sulfate contents of SFA of up to 1.8% SO_3 of SFA compared with the 0.55%–0.87% SO_3 of Class F FA. Alkalis were reported to have an influence on the setting times of FA-based concrete because they commonly hasten the setting time. Moreover, a relatively large alkali content could even result in an impressive set. The alkali content is of equal volume as the sodium oxide of SFA (i.e., 1.80), which may be attributed to the highly delayed setting of SFA. As the SFA levels increased, the blend paste began to harden. In particular, the strengths of the SFA-based concrete slightly decreased, thereby delaying the setting time of the cement when the ammoniated SFA was used because of the influences of the hostile sulfate and ammonium ions. For all levels of the SFA replacement for OPC in the SFA-based concrete, the final and initial even setting times of concrete increased in comparison with those of the reference mix. However, the length of delay in setting was slightly diverse in each level of SFA substitutions. The increase in the initial time of setting ranged from 15 min to 4 h and 45 min and that in the final setting time was from 1 h to 5 h and 25 min (see Table 1 and Fig. 8). In general, the increasing volume of SFA causes no change in the OPC content and could even lead to further delay in the setting time of SFA-based concrete. Several studies on another source of SFA-based concretes with higher than 50% SFA were conducted, which indicated a high reduction in all strengths of SFA-based concretes with large SFA levels.

3.2. Thermal profile

The thermal performance of all the mixtures was assessed by exposing the SFA-based concrete mortars to various temperatures (i.e., 100 °C, 300 °C, 500 °C, 700 °C, 900 °C, and 1000 °C). The weight loss in the different mixtures at 300 °C was approximately 13.2%, which may be attributed to water surface evaporation in the voids, physical binding of water to the reaction outputs, and partial sublimation of carbon afforded by SFA [75]. At elevated heats, this reduction is ascribed to the thirst

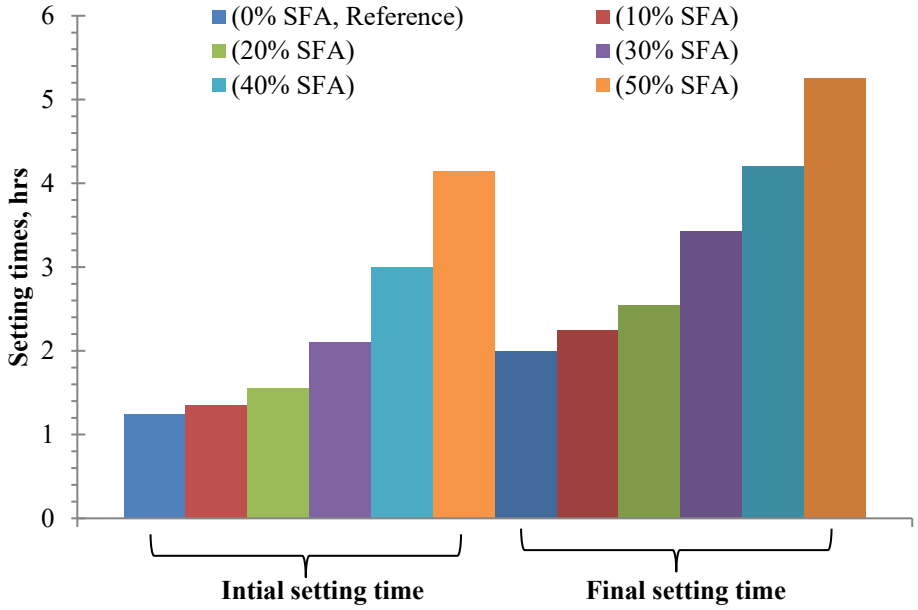

Fig. 8. Delay of the final and initial setting times of OPC/SFA-based concrete mortars.

procedure of the microstructure of geopolymer concretes [76–78] and decay of the calcium and sodium carbonates recognized by XRD. At 1000 °C, the weight losses for all the mixture systems assessed differed by nearly 2% between the 10% and 50% SFA-based concretes, which could be related to the mineral content in the used cement. This finding is according to the chemical composition of the cement presented in Table 1. The integration of 50% cement into the mix contributed to a 1.23% loss in ignition, leading to be nearly equal to the carbon dioxide of the decay of existing limestone in the used cement fraction. In volumetric alteration of the type of materials used, expansion and contraction alterations happened. The physical presence of the samples at 1000 °C enhanced the transition of a bushy mass into a permeable structure with a sponge-like manifestation (see Fig. 9, SEM). The findings of hardened strengths of the mixtures were 39.2 MPa and 26.5 MPa at 28 remedy days for the 10% and 50% SFA concrete mortars, respectively. After heating at 500 °C and up to 700 °C, an increase in strength of 14.4% was noticed in the FA-based concrete, while a decrease of 9.3% was detected in the hybrid of SFA content. These findings are equivalent to those reported in another study [77]. At 1000 °C, the extreme extension of the tested specimens prevented the assessment of the hardened strength and showed no cracks in the microstructure (Fig. 9). Another investigation of performance with the hollow particles present in the SFA, easing the stampede of the evaporation of water, and hence reducing intensive cracking in the microstructure [77,79]. Heating at different temperature rates could contribute to modifying the color of the tested specimens to gray with minor red points, which were detected in the mixtures containing more than 40% of SFA. The tested samples encompassing 100% SFA-based concrete showed an orange color, which is attributed to iron oxidation and carbon loss [80–84]. For clarity, when the levels of SFA replacement increased, the rate of the temperature decreased, and the color changed significantly, and vice versa.

3.3. Microstructure profile

Fig. 10 shows that the early strength of the SFA-based concrete mortars was lesser than that of the OPC-based concrete mortars. However, the majority of concrete mortars gained their strength after 28 days and above. This variation in strength may be attributed to the degree of fineness of the SFA contents. However, the sorptivity and SEM images show that the high fineness of SFA contents enhanced the porosity and microstructure of the mortars matrix. An elastic correlation was detected between the degree of hydration and the strength. The strength development of the SFA-based concrete mortars may be estimated on the basis of the mere distribution of the particle size of the used SFAs. Meanwhile, a small effect of the chemical composition of SFA on the cement hydration and strength development was detected. At 90 days, the samples were tested and passed through a 180-μm sieve and subsequently alienated into small cubes and positioned in the SEM mold for investigation. Several studies have examined cement hydration products, including their reactions through thermal analysis, SEM, and XRD [85]. XRD was utilized to classify the stages in the pastes hydrated with SFA. For example, the CaO/SiO_2 hydrate was the chief hydration product, which aids in the development of strength and microstructure binding. The ratio of Ca/Si in hydrated OPC was slightly adjustable, limited to the range of 0.75–2.15 and dependent on the cement composition, SFA, and description technique used [86]. In general, the degree of fineness of SFA can raise the microstructure of the SFA-based concrete, thereby leading to hardened strengths, reduced porosity, reduced sorptivity, and improved impermeability of the mass. Fig. 11 demonstrates that the main crystalline phases are mullite and quartz. The presence of a large percentage of aluminosilicate glassy phase (mullite) in SFA is mainly caused by the rapid cooling at elevated temperature. The ratio of alumina to silica of the present mullite is approximately 5.1:2.2. Mullite is a chemical substance added into the SFA-based concrete mortar. The XRD pattern of SFA implies that the remaining crystalline phase is hematite (CaO and Fe_2O_3). Hematite, mullite, and quartz are denoted by H, M, and Q, respectively. The relatively low intensity of CaO in the XRD pattern verifies the insignificant presence of Ca in the SFA specimens. Consistent with the ACI code, the presence of CaO, hematite, and quartz upsurges the strength and enhances the durability of the SFA-based concrete mortars.

Furthermore, the presence of low CaO content in the proportions of SFA-based concrete mortars lowers the strength and delays the development compared with a high CaO content. Hence, 50% SFA-based concrete mortar has a higher intensity (1043 cps at 29.3°) than the 100% SFA-based concrete mortar (47 cps).

3.4. Compressive strength

Fig. 12 shows the average compressive strength of the SFA-based concrete mortars versus the time of testing (i.e., after 3, 14, 28, 56, and 91 days and at 1 year). At 3 and 28 days, the reference mortar B00 (0%

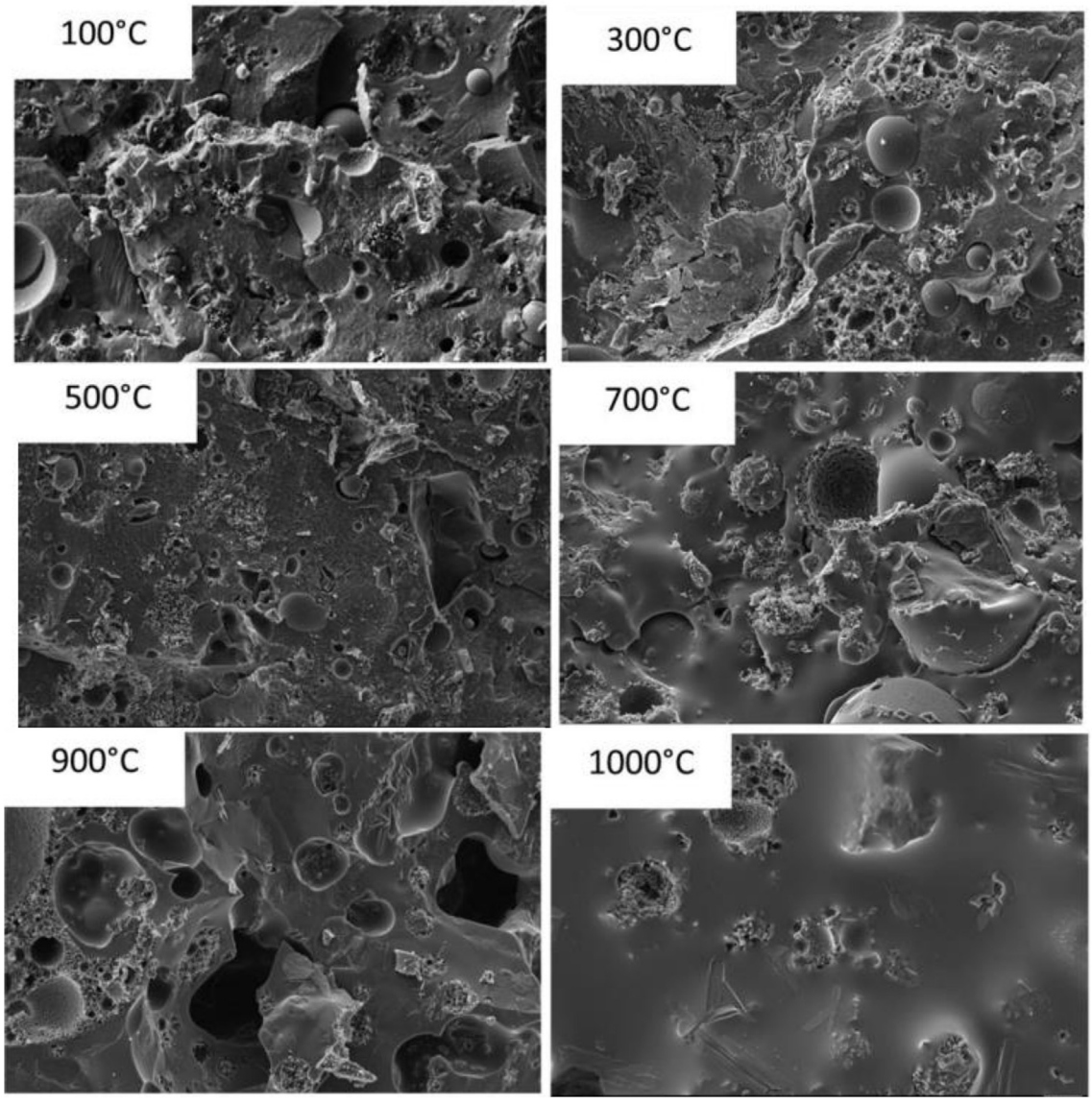

Fig. 9. Micrographs using SEM for the SFA-based concrete exposed to varied temperatures.

SFA) attained average compressive strengths of 14.3 and 42.4 MPa, with a standard deviation (SD) of 0.55 and 2.91, respectively, and a coefficient of variation (CV) of 3.86% and 6.87%, accordingly. On the other hand, mortars B10 (10% SFA), B20 (20% SFA), B30 (30% SFA), B40 (40% SFA), B50 (50% SFA) achieved average compressive strengths of (13.1 (SD = 1.00, CV = 7.63%) and 32.9 (SD = 2.97, CV = 9.05%)), (10.9 (SD = 0.60, CV = 5.50%) and 34.4 (SD = 3.14, 9.13%)), (8.30 (SD = 0.21, CV = 2.52%) and 31.3 (SD = 0.85, CV = 2.71%)), (6.8 (SD = 0.75, CV = 10.98%) and 28.8 (SD = 2.00, CV = 6.94%)), and (6.10 (SD = 0.90, CV = 14.61%) and 26.5 (SD = 1.00, CV = 3.77%)) MPa, respectively. These results indicate reductions of (8.39% and 7.55%), (23.78% and 18.40%), (41.96% and 26.18%), (52.45% and 32.08%), and (57.34% and 37.50%), respectively, compared to the strength of the reference mortar B00 (0% SFA). The findings at 56 days, 91 days and 1 year showed a substantial development in strength after 28 days. However, the enhancement in compressive strength was limited between 14.62% and 29.43% from 28 to 56 days, between 20.75% and 38.49% from 28 to 91 days, and between 32.78% and 43.45% from 28 days to 1 year. The increments in compressive strength might have occurred due to the sustained hydration of OPC. This considerable upsurge in strength of high-proportion SFA-based concrete is also caused by the pozzolanic reaction of SFA. At 3, 14, 28, 56, and 91 days and 1 year, the partial substitution of 50% OPC with SFA reduced the concrete compressive strength by 57.34%, 41.61%, 37.50%, 29.42%, 28.32%, and 35.52%, respectively (Fig. 12). Nonetheless, the compressive strengths indicated that even mortars B40 (40% SFA) and B50 (50% SFA) can continue to be potentially utilized for fabricating structural concrete elements, including precast concrete, in the construction industry.

3.5. Flexural strength

Fig. 13 presents the average flexural strength of the SFA-based concrete mortars versus the time of testing (i.e., after 3, 14, 28, 56, and 91 days and 1 year). The average flexural strength followed a similar trend to the average compressive strength (i.e. decreased by increment of SFA and increased by age). At 3, 28, and 91 days, reference mortar B00 (0% SFA) attained flexural strengths of 3.1 (SD = 0.25, CV = 8.03%), 5.2 (SD = 0.6, CV = 11.54%), and 5.8 kN (SD = 0.15, CV = 2.65%), whereas mortars B10 (10% SFA), B20 (20% SFA), B30 (30% SFA), B40 (40% SFA), and B50 (50% SFA) have achieved flexural strengths of (2.9 (SD = 0.2, CV = 6.90%), 4.6 (SD = 0.45, CV = 9.73%), and 5.5 (SD = 0.4, CV = 7.27%)), (2.6 (SD = 0.46, CV = 17.54%), 4.4 (SD = 0.55, CV = 12.61%),

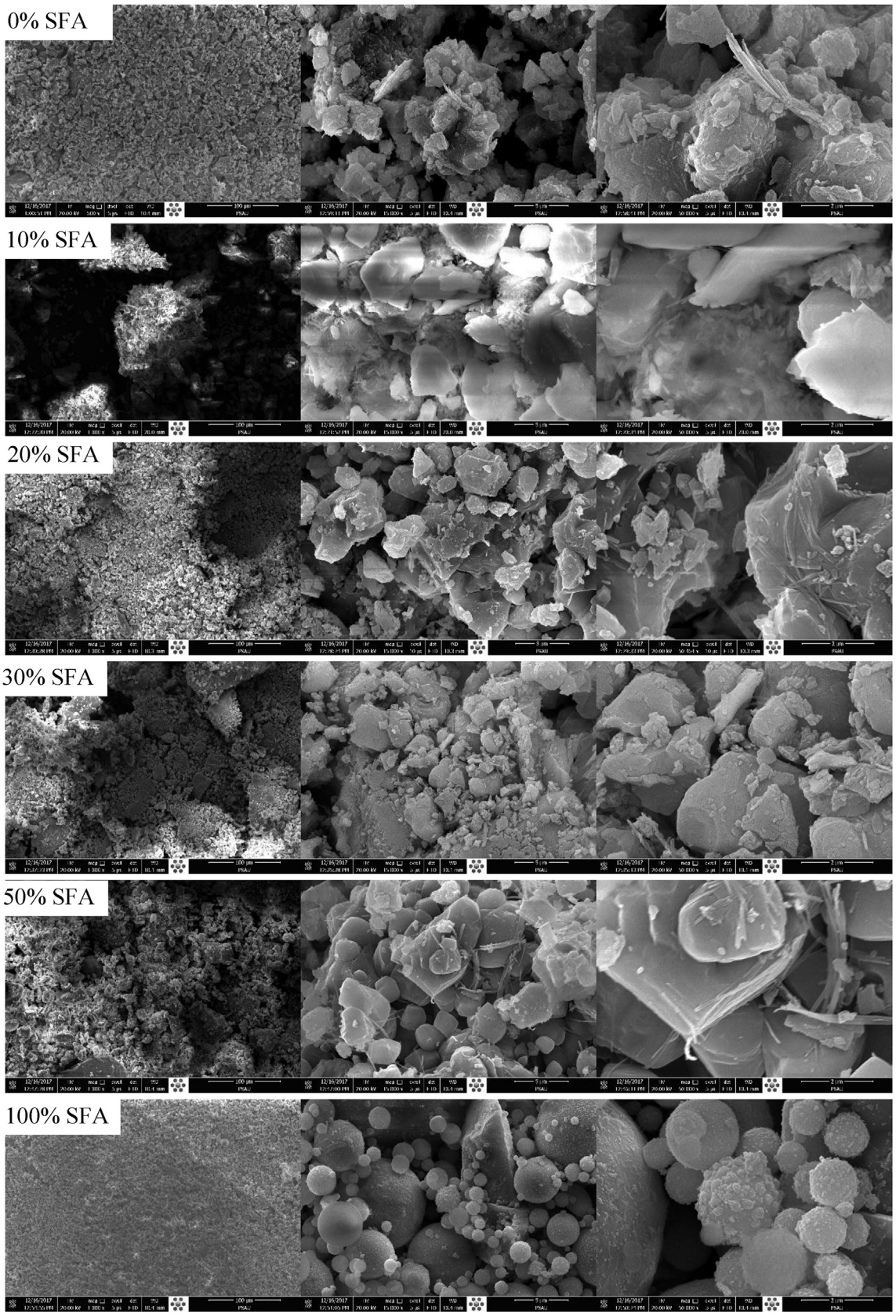

Fig. 10. SFA-based concrete samples via SEM images.

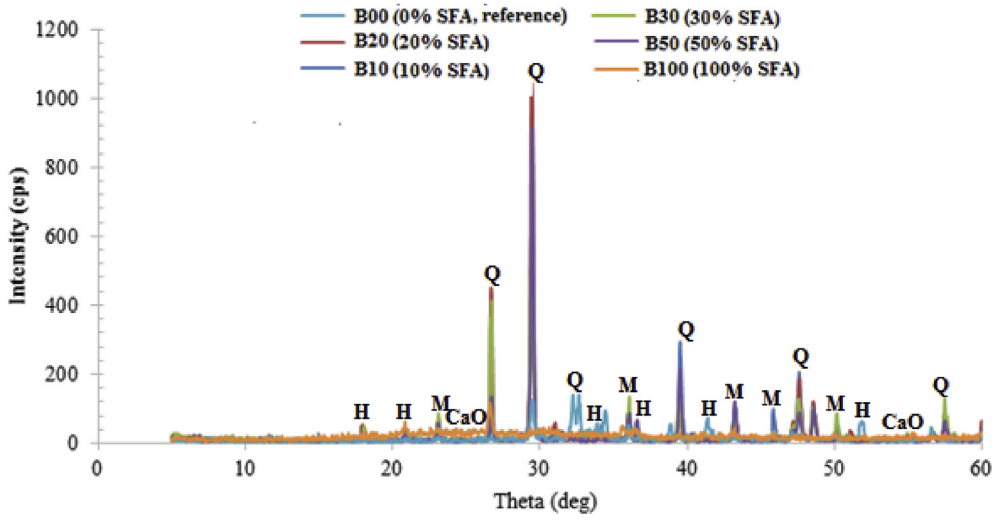

Fig. 11. XRD profiles of OPC/SFA-based concrete.

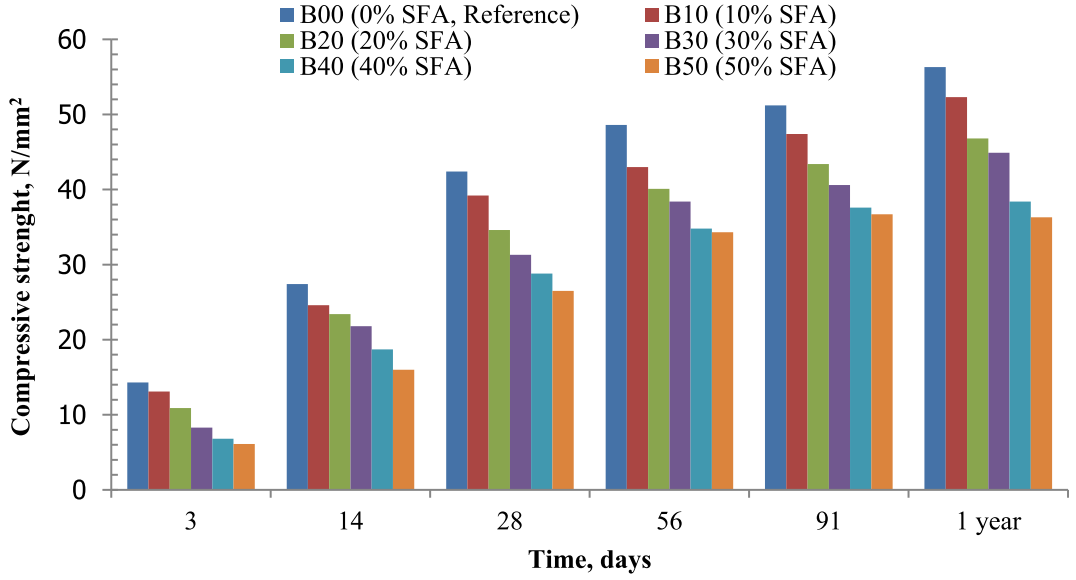

Fig. 12. Compressive strength vs. time of testing.

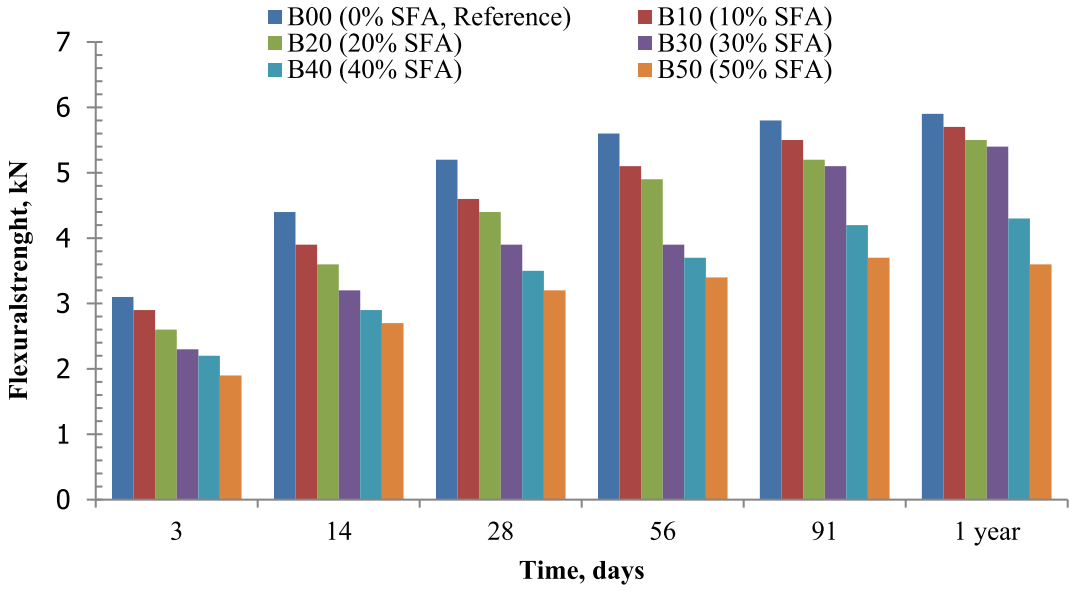

Fig. 13. Flexural strength vs. time of testing.

and 5.2 (SD = 1.00, CV = 19.23%)), (2.3 (SD = 0.06, CV = 2.47%), 3.9 (SD = 1.00, CV = 25.64%), and 5.1 (SD = 0.65, CV = 12.67%)), (2.2 (SD = 0.29, CV = 12.93%), 3.5 (SD = 0.67, CV = 19.21%), and 4.2 (SD = 0.65, CV = 15.62%)), and (1.9 (SD = 0.70, CV = 36.84%), 3.2 (SD = 0.4, CV = 12.50%), and 3.7 (SD = 0.57, CV = 15.23%)) kN, respectively; that is reductions of (6.45%, 11.54%, and 5.17%), (16.13%, 15.38%, and 10.34%), (35.81%, 25.00%, and 12.07%), (29.03%, 32.69%, and 27.59%), and (38.71%, 38.46%, and 36.21%) when compared to the strengths of the reference mortar B00 (0% SFA), respectively. This substantial increment in flexural strength of high-proportion SFA-based concrete may be caused by the pozzolanic reaction of SFA and continuous hydration of OPC. After 3, 14, 28, 56, and 91 days and 1 year, the partial substitution of OPC with SFA (from 10% to 50%) condensed the flexural strength of concrete by 34.48%, 30.77%, 30.43%, 33.33%, 32.73%, and 36.84%, respectively (see Fig. 13). The findings also show that continuous flexural strength development was maintained, even beyond 28 days. The increase in flexural strength of 30% SFA-based concretes from 28 to 91 days and from 28 to 1 year were up by 30.77% and 38.46%, respectively.

3.6. Splitting tensile strength

Fig. 14 illustrates the STS of SFA-based concrete mortars versus the time of testing (i.e., after 3, 14, 28, 56, and 91 days and 1 year). The trend seen in the STS against SFA content was also observed in the compressive and flexural strengths (i.e. the STS reduced with a rise in SFA content). At 3 and 28 days, the STSs of the reference mortar B00 (0% SFA) were 2.2 MPa (SD = 0.35, CV = 16.21%) and 5.5 MPa (SD = 0.38, CV = 6.84%), respectively, whereas mortars B10 (10% SFA), B20 (20% SFA), B30 (30% SFA), B40 (40% SFA), and B50 (50% SFA) exhibited STSs of (2.0 (SD = 0.20, CV = 10.00%) and 5.5 (SD = 0.35, CV = 6.42%)), (1.9 (SD = 0.20, CV = 10.53%) and 5.3 (SD = 0.35, CV = 6.67%)), (1.7 (SD = 0.20, CV = 11.76%) and 4.3 (SD = 0.55, CV = 12.71%)), (1.4 (SD = 0.44, CV = 31.33%) and 3.8 (SD = 0.42, CV = 10.86%)), and (1.2 (SD = 0.30, CV = 25.00%) and 2.9 (SD = 0.35, CV = 11.97%)) MPa, respectively; a reduction of (9.09% and 3.64%), (13.64% and 10.91%), (22.73% and 21.82%), (36.36% and 30.91%), and (45.45% and 47.37%), respectively, compared with the STS strength of the reference mortar B00 (0% SFA). However, STS was observed to continuously increase with time. At 56 and 91 days, mortars B00 (0% SFA), B10 (10% SFA), B20 (20% SFA), B30 (30% SFA), B40 (40% SFA), and B50 (50% SFA) attained STSs of (5.8 (SD = 0.45, CV = 7.73%) and 6.0 (SD = 0.4, CV = 7.01)), (5.5 (SD = 0.53, CV = 9.62%) and 5.7 (SD = 0.45, CV = 7.96%)), (5.1 (SD = 0.75, CV = 14.62%) and 5.3 (SD = 0.69, CV = 13.07%)), (4.4 (SD = 0.57, CV = 12.83%) and 4.6 (SD = 0.5, CV = 10.87%), (4.0 (SD = 0.42, CV = 10.32%) and 4.3 (SD = 0.57, CV = 13.33%)), and (3.1 (SD = 0.25, CV = 8.03%) and 3.2 (SD = 0.4, CV = 12.50%)) MPa, respectively, thereby showing increases of (5.45% and 9.09%), (3.77% and 7.55%), (4.08% and 8.16%), (2.33% and 6.98%), (5.26% and 13.16%), and (6.90% and 10.34%), respectively, compared with the values recorded at the 28th-day STS strength. The increase in the 1-year STS values with the increasing percentage of SFA in the B00 (0% SFA), B10 (10% SFA), B20 (20% SFA), B30 (30% SFA), B40 (40% SFA), and B50 (50% SFA) when compared to the 28th-day STS strength were 23.64%, 16.98%, 12.24%, 9.30%, 18.42%, and 13.79%, respectively. The attained results reveal that the ratio of increment in STS strengths at 91 days and 1 year from 28-days was considerably high for the SFA-based concrete mortars and reference mortar. This could be due to the active pozzolanic reactions in the SFAs.

3.7. Modulus of elasticity

This study adopted the modulus of elasticity (MoE) as the secant modulus on the basis of a common scientific term and considered a descending string from the radix to a particular spot point on the stress–strain relationship curve. However, the secant modulus computed in this investigation was approximately 36.3% of the highest stress peak point. MoEs of the SFA-based concrete mortars were measured at interval periods of 3, 14, 28, 56, and 91 days and 1 year. Fig. 15 illustrates the MoE of SFA-based concrete mortars versus the time of testing (i.e., at 3, 14, 28, 56, and 91 days and 1 year). The experimental investigation results display that the use of high-proportion SFA condensed the MoE of the SFA-based concrete mortars when compared with that of the reference mortar. At 28 days and 1 year, reference mortar B00 (0% SFA) obtained MoEs of 30.2 GPa (SD = 2.00, CV = 6.62%) and 31.6 GPa (SD = 0.65, CV = 2.06%), respectively, whereas mortars B10 (10% SFA), B20 (20% SFA), B30 (30% SFA), B40 (40% SFA), and B50 (50% SFA) obtained MoEs of (27.8 (SD = 1.94, CV = 6.97%) and 31.5 (SD = 0.67, CV = 2.12%)), (24.5 (SD = 1.91, CV = 7.79%) and 30.0 (SD = 1.29, CV = 4.29%)), (22.9 (SD = 1.19, CV = 5.22%) and 27.1 (SD = 1.79, CV = 6.60%)), (20.8 (SD = 2.10, CV = 10.13%) and 23.9 (SD = 2.00, CV = 8.37%)), and (19.0 (SD = 1.50, CV = 7.90%) and 22.1 (SD = 0.95, CV = 4.29%)) GPa, respectively. Moreover, at 56 and 91 days and 1 year, the findings showed that the MoE of SFA-based concrete mortars continuously increased with the time.

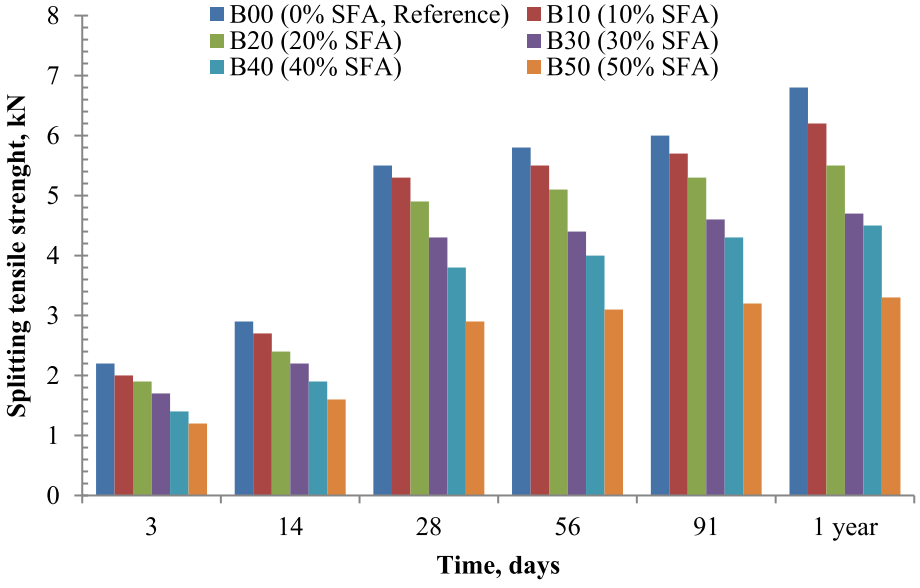

Fig. 14. Splitting tensile strength vs. time of testing.

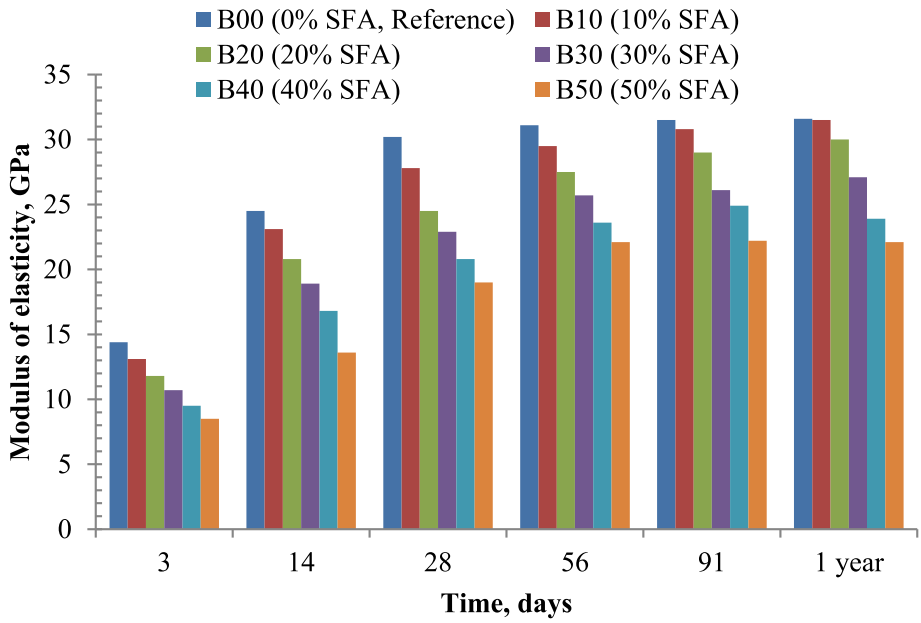

Fig. 15. Modulus of elasticity vs. time of testing.

3.8. Depth of wear penetration

Fig. 16 shows the variation of the wear depth of the SFA-based concrete mortars versus the time of testing (i.e., 3, 14, 28, 56, and 91 days and 1 year after) under 1 h of abrasion. The results reveal that the wear depth of OPC-based concrete mortar B00 (0% SFA) containing zero SFA was higher than those of SFA-based concrete mortars B10 (10% SFA), B20 (20% SFA), B30 (30% SFA), B40 (40% SFA), and B50 (50% SFA) that comprise 10%, 20%, 30%, 40%, and 50% SFA, respectively. At 28 days and 1 year, the wear depths of mortars B00 (0% SFA), B10 (10% SFA), B20 (20% SFA), B30 (30% SFA), B40 (40% SFA), and B50 (50% SFA) were (3.02 (SD = 0.10, CV = 3.31%) and 2.52 (SD = 0.17, CV = 6.87%)), (2.88 (SD = 0.18, CV = 6.22%) and 2.42 (SD = 0.10, CV = 4.13%)), (2.72 (SD = 0.20, CV = 7.35%) and 2.36 (SD = 0.20, CV = 8.47%)), (2.41 (SD = 0.20, CV = 8.30%) and 2.28 (SD = 0.10, CV = 4.18%)), (2.01 (SD = 0.06, CV = 2.74%) and 2.21 (SD = 0.11, CV = 4.75%)), and (1.51 (SD = 0.10, CV = 6.62%) and 1.96 (SD = 0.05, CV = 2.57%) mm, respectively. The wear depths decreased from 28 days to 1 year by approximately 16.56%, 15.97%, 13.24%, and 5.39% when SFA addition increased by 0%, 10%, 20%, and 30%, respectively. Thereafter, the wear depths increased from 28 days to 1 year by nearly 9.95% and 29.80% when SFA increased to 40% and 50%, respectively. The results indicated that the wear depth could substantially increase when the added volume of SFA exceeds 40% of OPC substitution.

3.8.1. Abrasion resistance

Figs. 17 and 18 demonstrate the variation of abrasion resistance of the SFA-based concrete mortars versus the time of testing at 28 days and 1 year under 70 min of abrasion. The test findings showed that the abrasion resistance values of concrete mortars B10 (10% SFA), B20 (20% SFA), B30 (30% SFA), B40 (40% SFA), and B50 (50% SFA) that comprise 10%, 20%, 30%, 40%, and 50% SFA, respectively, were less than that of the

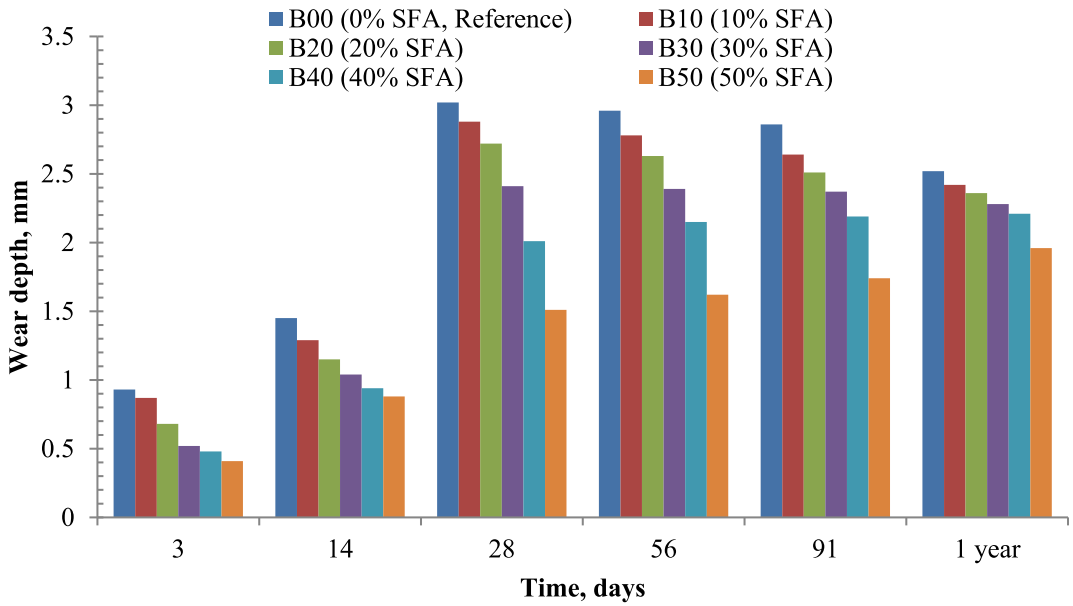

Fig. 16. Wear depth at 1 h of abrasion.

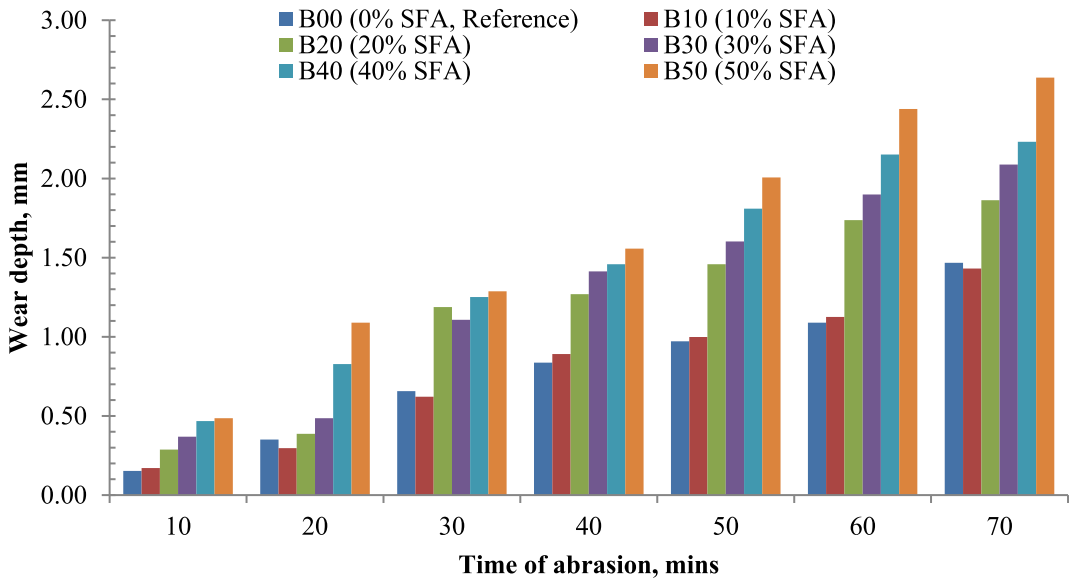

Fig. 17. Wear depth vs. time of abrasion at 28 days.

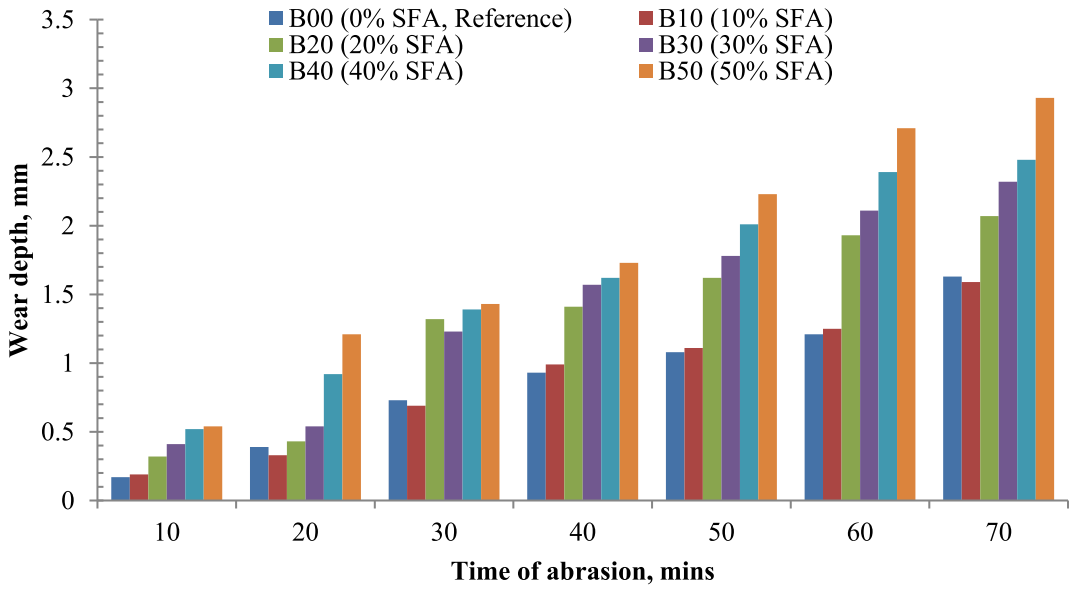

Fig. 18. Wear depth vs. time of abrasion at 1 year.

reference mortar B00. At 28 days and 1 year, the wear depths for mortars B00 (0% SFA), B10 (10% SFA), B20 (20% SFA), B30 (30% SFA), B40 (40% SFA), and B50 (50% SFA) were (1.47 (SD = 0.02, CV = 1.19%) and 1.63 (SD = 0.03, CV = 2.13%)), (1.43 (SD = 0.02, CV = 1.40%) and 1.59 (SD = 0.15, CV = 9.26%)), (1.86 (SD = 0.003, CV = 0.19%) and 2.07 (SD = 0.04, CV = 1.93%)), (2.09 (SD = 0.02, CV = 0.83%) and 2.32 (SD = 0.11, CV = 4.54%)), (2.23 (SD = 0.01, CV = 0.47%) and 2.48 (SD = 0.01, CV = 0.23%)), and (2.64 (SD = 0.01, CV = 0.53%) and 2.93 (SD = 0.09, CV = 3.13%)) mm, respectively. The difference of the abrasion resistance with period of times for all SFA-based concrete mortars at ages 3, 14, 56, and 91 days produced the same results as those at 28 days and 1 year. Therefore, wear depth increased with the extension of the abrasion time for all mortars. All strengths, particularly compressive strength, significantly influenced the abrasion resistance of the SFA-based concrete.

4. Conclusions

This research paper presents the performance properties of high-proportion SFA-based concrete at different times of testing (i.e., 3, 14, 28, 56, and 91 days and 1 year). The use of SFA as a suitable SCM to partly substitute cement in the fabrication of SFA-based concrete is crucial. To increase the SFA levels, an extensive experimental work was carried out to utilize SFA in the production of concrete. Six concrete mixes were utilized: five out of the six mixes were prepared with different SFA levels and one mix was used as the reference. This research presents the findings of adding high volumes of SFA at different proportions (i.e., 0%, 10%, 20%, 30%, 40%, and 50%). Experimental tests were performed on the properties of SFA-based concrete, including slump test, air content, setting times, thermal profile, specific gravity, sieve gradation, flexural strength, tensile strength, compressive strength, wear, resistance to abrasion, and elasticity modulus, at different time intervals for one year. The subsequent conclusions were observed on the bases of the major results of this study.

- The substitution of OPC with five proportions of SFA condensed all strengths, including MoE of SFA-based concrete at 28 days of testing

time. However, an incessant and considerable development of strength properties was still observed after 28 days.

- The strengths of the SFA-based concrete with 10%, 20%, 30%, 40%, and 50% SFA contents after 28 days were found to be adequate for the fabrication of structural concrete elements in the construction industry.
- The wear depth was also highest 1 h after abrasion for all SFA-based concrete mortars.
- The resistance to abrasion of the FA-based concrete was substantially affected by its hardened strength, regardless of the SFA content. Meanwhile, the resistance to abrasion improved with the increment in age for all SFA-based concrete mortars.
- SFA has emerged as a new engineering material, contributing towards environmentally sustainable construction and building products, at construction industries today.

Further investigations are recommended, such as the enhancement of the durability and strength of SFA in the hardened state using fibers and the exploration of the potential application of FA in the construction of green buildings and forthcoming sustainable cities with a reduced carbon footprint.

Acknowledgment

The authors gratefully acknowledge the financial support of the Department of Civil Engineering, College of Engineering, Prince Sattam Bin Abdulaziz University, Saudi Arabia; the Department of Civil Engineering, Faculty of Engineering, Amran University, Yemen, and the valuable guidance and supervision by the Structural Impact Laboratory (SIMLab), Department of Structural Engineering, Norwegian University of Science and Technology, Norway; for this research.

References

[1] K. Celik, C. Meral, A.P. Gursel, P.K. Mehta, A. Horvath, P.J. Monteiro, Mechanical properties, durability, and life-cycle assessment of self-consolidating concrete mixtures made with blended portland cements containing fly ash and limestone powder, Cement Concr. Compos. 56 (2015) 59–72.
[2] F.U.A. Shaikh, Mechanical and durability properties of fly ash geopolymer concrete containing recycled coarse aggregates, Int. J. Sustain. Built Environ. 5 (2) (2016) 277–287.
[3] M.B. S, B.R.C., V.K., Strength behaviour of geopolymer concrete replacing fine aggregates by M- sand and, E-waste Int. J. Eng. Trends Technol. (IJETT) 4 (7) (2016) 401–407.
[4] R. Lakshmi, S. Nagan, Utilization of waste E plastic particles in cementitious mixtures, J. Struct. Eng. 38 (1) (2011) 26–35.
[5] C. Madheswaran, G. Gnanasundar, N. Gopalakrishnan, Effect of molarity in geopolymer concrete, Int. J. Civ. Struct. Eng. 4 (2) (2013) 106.
[6] Garside, M. Largest coal consumption worldwide by country 2018. Statista (9 Aug 2019), rereived from https://www.statista.com/statistics/265510/countries-with-the-largest-coal-consumption/on 11 March 2020.
[7] A. Castel, Bond between Steel Reinforcement and Geopolymer Concrete, Handbook of Low Carbon Concrete, 2016, p. 375.
[8] M.A. G. Gurunarayanan Shalini, S. Sakthivel, Performance of rice husk ash in geopolymer concrete, Int. J. Innov. Res. Sci. Technol. 2 (12) (2016).
[9] J. Davidovits, 30 years of successes and failures in geopolymer applications. Market trends and potential breakthroughs. Keynote Conference on Geopolymer Conference, 2002.
[10] J.S. Joy, M. Mathew, Experimental study on geopolymer concrete with partial replacement of fine aggregate with foundry sand, Int. J. Adv. Technol. Eng. Sci. 3 (1) (2015).
[11] W. Li, J. Xu, Mechanical properties of basalt fiber reinforced geopolymeric concrete under impact loading, Mater. Sci. Eng. 505 (1) (2009) 178–186.
[12] K. Soltaninaveh, The Properties of Geopolymer Concrete Incorporating Red Sand as Fine Aggregate, Thesis of Master of engineering, Curtin University of Technology, Australia, 2008.
[13] B.S. Thomas, S. Kumar, H.S. Arel, Sustainable concrete containing palm oil fuel ash as a supplementary cementitious material–A review, Renew. Sustain. Energy Rev. 80 (2017) 550–561.
[14] M.F. Awalludin, O. Sulaiman, R. Hashim, W.N.A.W. Nadhari, An overview of the oil palm industry in Malaysia and its waste utilization through thermochemical conversion, specifically via liquefaction, Renew. Sustain. Energy Rev. 50 (2015) 1469–1484.
[15] M.T. Marvila, J. Alexandre, A.R.G. Azevedo, E.B. Zanelato, G.C. Xavier, S.N. Monteiro, Study on the replacement of the hydrated lime by kaolinitic clay in mortars, Adv. Appl. Ceram. 118 (7) (2019) 373–380.
[16] B.A. Silva, A.P.F. Pinto, A. Gomes, Influence of natural hydraulic lime content on the properties of aerial lime-based mortars, Construct. Build. Mater. 72 (2018) 208–218.
[17] L.P. Junior, F. Brennand, A.J.C. Silva, et al., Study on the quality of lime produced in Pernambuco and its influence on mortars, Ambiente Construído 11 (2006) 4299–4308.
[18] A. Dowling, J. O'Dwyer, C.C. Adley, Lime in the limelight, J. Clean. Prod. 92 (2015) 13–22.
[19] A.R.G. Azevedo, M.T. Marvila, L.S. Barroso, E.B. Zanelato, J. Alexandre, G.C. Xavier, S.N. Monteiro, Effect of granite residue incorporation on the behavior of mortars, Materials 12 (2019) 1449.
[20] J. Alexandre, A.R.G. Azevedo, G.C. Xavier, L.G. Pedroti, C.M.F. Vieira, S.N. Monteiro, Characterization of a limestone powder residue for recycling as a concrete block incorporation, Mater. Sci. Forum 798–799 (2014) 3–8.
[21] A.R.G. Azevedo, J. Alexandre, G.C. Xavier, V.S. Candido, S.N. Monteiro, C.M.F. Vieira, Relevance of ornamental stone residues in the manufacture of concrete blocks for structural masonry, Mater. Sci. Forum 798–799 (2014) 638–643.
[22] M. Gatto, M. Wollni, M. Qaim, Oil palm boom and land-use dynamics in Indonesia: the role of policies and socioeconomic factors, Land Use Pol. 46 (2015) 292–303.
[23] Y.H. Mugahed Amran, R. Alyousef, H. Alabduljabbar, M. El-Zeadani, Clean production and properties of geopolymer concrete; A review, J. Clean. Prod. 251 (2020), 119679.
[24] N. O. Sulaiman, S. Nurjannah, N. Afeefah, R. Hashim, I. Mazlan, M. Sato, The potential of oil palm trunk biomass as an alternative source for compressed wood BioResources 7 (2) (2012) 2688–2706.
[25] F. Abutaha, H.A. Razak, J. Kanadasan, Effect of palm oil clinker (POC) aggregates on fresh and hardened properties of concrete, Construct. Build. Mater. 112 (2016) 416–423.
[26] A. Abdullah, B. Zuhairi, H.M. Salamatinia, S. Bhatia, Current status and policies on biodiesel industry in Malaysia as the world's leading producer of palm oil, Energy Pol. 37 (12) (2009) 5440–5448.
[27] Aim, National Biomass Strategy 2020: New Wealth Creation for Malaysia's Palm Oil Industry, Cyberjaya MY: Agensi Inovasi Malaysia, November, 2011, p. 32.
[28] Al-mulali, M. Zuhear, A. Hanizam, H.P.S.A. Khalil, S.A. Zaid, The incorporation of oil palm ash in concrete as a means of recycling: a review, Cement Concr. Compos. 55 (2015) 129–138.
[29] B. Alsubari, S. Payam, M. Zamin, U. Johnson, A. Palm oil fuel ash as a partial cement replacement for producing durable self-consolidating high-strength concrete, Arabian J. Sci. Eng. 39 (12) (2014) 8507–8516.
[30] B. Alsubari, P. Shafigh, M.Z. Jumaat, Utilization of high-volume treated palm oil fuel ash to produce sustainable self-compacting concrete, J. Clean. Prod. 137 (2016) 982–996.
[31] J.P. Hwang, B.S. Hyun, S. Lim, Y. Ki, Ann. Enhancing the durability properties of concrete containing recycled aggregate by the use of pozzolanic materials, KSCE J. Civil Eng. 17 (1) (2013) 155–163.
[32] G.C. Isaia, A.L.G. Gastaldini, R. Moraes, Physical and pozzolanic action of mineral additions on the mechanical strength of high-performance concrete, Cement Concr. Compos. 25 (1) (2003) 69–76.
[33] S.R. Sumadi, M.W. Hussin, Palm oil fuel ash (POFA) as a future partial cement replacement material in housing construction, J. Ferrocem. 25 (1) (1995) 25–34.
[34] A.A. Awal, M.W. Hussin, The effectiveness of palm oil fuel ash in preventing expansion due to alkali-silica reaction, Cement Concr. Compos. 19 (4) (1997) 367–372.
[35] A. Awal, M.W. Hussin, Durability of high performance concrete containing palm oil fuel ash, in: Proceedings of Eighth International Conference on the Durability of Building Materials and Components, British Columbia, Vancouver, 1999. Canada.
[36] P. Chindaprasirt, S. Homwuttiwong, C. Jaturapitakkul, Strength and water permeability of concrete containing palm oil fuel ash and rice husk–bark ash, Construct. Build. Mater. 21 (7) (2007) 1492–1499.
[37] C. Jaturapitakkul, K. Kraiwood, T. Weerachart, S. Tirasit, Evaluation of the sulfate resistance of concrete containing palm oil fuel ash, Construct. Build. Mater. 21 (7) (2007) 1399–1405.
[38] V. Sata, C. Jaturapitakkul, K. Kiattikomol, Influence of pozzolan from various by-product materials on mechanical properties of high-strength concrete, Construct. Build. Mater. 21 (7) (2007) 1589–1598.
[39] W. Tangchirapat, C. Jaturapitakkul, P. Chindaprasirt, Use of palm oil fuel ash as a supplementary cementitious material for producing high-strength concrete, Construct. Build. Mater. 23 (7) (2009) 2641–2646.
[40] J. Wood, R. Johnson, The appraisal and maintenance of structures with alkali-silica reaction, Struct. Eng. 71 (2) (1993).
[41] S.H. Ghaffar, M. Al-Kheetan, P. Ewens, T. Wang, J. Zhuang, Investigation of the interfacial bonding between flax/wool twine and various cementitious matrices in mortar composites, Construct. Build. Mater. 239 (2020) 117833.
[42] M.J. Al-Kheetan, M.M. Rahman, D.A. Chamberlain, Optimum mix design for internally integrated concrete with crystallizing protective material, J. Mater. Civ. Eng. 31 (7) (2019), https://doi.org/10.1061/(ASCE)MT.1943-5533.0002694.
[43] M.J. Al-Kheetan, M.M. Rahman, Integration of anhydrous sodium acetate (ASAc) into concrete pavement for protection against harmful impact of deicing salt, JOM 71 (2019) 4899–4909, https://doi.org/10.1007/s11837-019-03624-3.
[44] U.J. Alengaram, B.A. Al Muhit, M.Z. bin Jumaat, Utilization of oil palm kernel shell as lightweight aggregate in concrete–a review, Construct. Build. Mater. 38 (2013) 161–172.
[45] U.J. Alengaram, A. Baig, M. Al Muhit, J. Zamin, , and Michael L. Y. Jing A comparison of the thermal conductivity of oil palm shell foamed concrete with conventional materials, Mater. Des. 51 (2013) 522–529.

[46] M. Aldahdooh, N.M. Bunnori, M.M. Johari, Development of green ultra-high performance fiber reinforced concrete containing ultrafine palm oil fuel ash, Construct. Build. Mater. 48 (2013) 379–389.
[47] S.O. Bamaga, M.A. Ismail, Z.A. Majid, M. Ismail, M.W. Hussin, Evaluation of sulfate resistance of mortar containing palm oil fuel ash from different sources, Arabian J. Sci. Eng. 38 (9) (2013) 2293–2301.
[48] V. Sata, A. Sathonsaowaphak, P. Chindaprasirt, Resistance of lignite bottom ash geopolymer mortar to sulfate and sulfuric acid attack, Cement Concr. Compos. 34 (5) (2012) 700–708.
[49] V. Sata, A. Wongsa, P. Chindaprasirt, Properties of pervious geopolymer concrete using recycled aggregates, Construct. Build. Mater. 42 (2013) 33–39.
[50] S.M. Kabir, U. Johnson A, M. Zamin J, S. Afia, A. Islam, Influence of molarity and chemical composition on the development of compressive strength in POFA based geopolymer mortar, Adv. Mater. Sci. Eng. 5 (1) (2015) 1–15.
[51] Optimization of the EMI shielding effectiveness of fine and ultrafine POFA powder mix with OPC powder using Flower Pollination Algorithm, in: IOP Conference Series: Materials Science and Engineering, IOP Publishing, 2017.
[52] M.H. Ahmad, R.C. Omar, M.A. Malek, N. Md Noor, S. Thiruselvam, Compressive strength of palm oil fuel ash concrete, Proc. Int. Conf. Construct. Build. Technol. 27 (2008) 297–306.
[53] S. Bamaga, M. Hussin, M.A. Ismail, Palm oil fuel ash: promising supplementary cementing materials, KSCE J. Civil Eng. 17 (7) (2013) 1708–1713.
[54] S.O. Bamaga, M.A. Ismail, M.W. Hussin, Chloride resistance of concrete containing palm oil fuel ash, Concr. Res. Lett. 1 (4) (2011) 158–166.
[55] I.I. Bashar, U. Johnson A, M. Zamin J, A. Islam, S. Helen, S. Afia, Engineering properties and fracture behaviour of high volume palm oil fuel ash based fibre reinforced geopolymer concrete, Construct. Build. Mater. 111 (2016) 286–297.
[56] M. Hussin, T. Ishida, A study on basic properties of hardened concrete containing palm oil fuel ash as partial cement replacement material, in: Proceedings of the Annual Meeting in Materials and Construction, Summaries of Technical, Architectural Institute of Japan, 1999.
[57] A.M. Neville, Properties of Concrete, Prentice Hall, 2000.
[58] Djwantoro Hardjito, B. Vijaya Rangan, Development and Properties of Low-Calcium Fly Ash-Based Geopolymer Concrete, Thesis, Curtin University, 2005.
[59] ASTM C 150, Standard Specification for Portland Cement. Philadelphia, Annual book ASTM International, West Conshohocken, PA, 2002, p. 4.
[60] ASTM C 311, Standard Test Methods for Sampling and Testing Fly Ash or Natural Pozzolans for Use in Portland-Cement Concrete, Philadelphia ASTM International, West Conshohocken, PA, 2002, p. 4.
[61] ASTM C 136, Standard Test Method for Sieve Analysis of Fine and Coarse Aggregates. Philadelphia, Annual book ASTM International, West Conshohocken, PA, 2002, 4(2).
[62] ASTM C 494, Standard Specification for Chemical Admixtures for Concrete. Philadelphia, Annual book ASTM International, West Conshohocken, PA, 1999, p. 4.
[63] ASTM C 618, Standard Specification for Fly Ash and Raw or Calcined Natural Pozzolan for Use as a Mineral Admixture in Portland Cement Concrete. Philadelphia, Annual book ASTM International, West Conshohocken, PA, 2003, p. 4.
[64] BS 882, 1992, Specification for Aggregate from Natural Resources for Concrete, British Standards Institution, London, 1992.
[65] ASTM C 403, Standard Test Method for Time of Setting of Concrete Mixtures by Penetration Resistance. Philadelphia, Annual book ASTM International, West Conshohocken, PA, 2008.
[66] ASTM C 127, Standard Test Method for density." Relative Density (Specific Gravity), and Absorption of Coarse Aggregate. Philadelphia, Annual book ASTM International, West Conshohocken, PA, 2007.
[67] ASTM C 31, Cast and Laboratory Cure Two Sets of Two Standard Cylinder Specimens for Each Composite Sample. B. Cast and Field Cure Two Sets of Two Standard Cylinder Specimens for Each Composite Sample. Philadelphia, Annual book ASTM International, West Conshohocken, PA, 2005.
[68] BS EN 12390-3, Testing Hardened Concrete. Compressive Strength of Test Specimens, 2009. May 31.
[69] ASTM C 143, Standard Test Method for Slump of Hydraulic Cement Concrete, ASTM International, West Conshohocken, PA, 1996, p. 4.
[70] ASTM C 39, Standard test method for compressive strength of cylindrical concrete specimens 4, Annual book of ASTM standards, 1996.
[71] ASTM C 496, Standard Test Method for Splitting Tensile Strength of Cylindrical Concrete Specimens, Philadelphia, Annual book ASTM International, West Conshohocken, PA, 2004.
[72] ASTM C 78, Standard Method for Flexural Strength of Concrete (Using Simple Beam with Third Point Loading. Philadelphia, Annual book ASTM International, West Conshohocken, PA, 2002.
[73] Astm C 469, Standard Test Method for Static Modulus of Elasticity and Poisson's Ratio of Concrete in Compression. Philadelphia, Annual book ASTM International, West Conshohocken, PA, 2002, p. 4.
[74] ASTM C 779, Standard Test Method for Abrasion Resistance of Horizontal Concrete Surfaces. Philadelphia, Annual book ASTM International, West Conshohocken, PA, 2002.
[75] D. Macphee, I. Garcia-Lodeiro, Activation of aluminosilicates - some chemical considerations, Proc. Slag Valorisation Symposium (2011) 51–61.
[76] A. Buchwald, M. Vicent, R. Kriegel, C. Kaps, M. Monzó, A. Barba, Geopolymeric binders with different fine fillers - phase transformations at high temperatures, Appl. Clay Sci. 46 (20) (2009) 190–195.
[77] D.L.Y. Kong, J.G. Sanjayan, Effect of elevated temperatures on geopolymer paste, mortar and concrete, Cement Concr. Res. 40 (2) (2010) 334–339.
[78] S. Donatello, C. Kuenzel, A. Palomo, A. Fernandez-Jimenez, High temperature resistance of a very high volume fly ash cement paste, Cement Concr. Compos. 45 (2014) 234–242.
[79] D.L.Y. Kong, J.G. Sanjayan, K. Sagoe-Crentsil, Comparative performance of geopolymers made with metakaolin and fly ash after exposure to elevated temperatures, Cement Concr. Res. 37 (12) (2007) 1583–1589.
[80] M. El-Zeadani, M.R. Saifulnaz, F. Hejazi, Y.M. Amran, M.S. Jaafar, R. Alyousef, F. Alrshoudi, Mechanics-based approach for predicting the short-term deflection of CFRP plated RC beams, Compos. Struct. 225 (2019) 111169.
[81] Y.M. Amran, R.S. Rashid, F. Hejazi, A.A. Ali, N.A. Safiee, S.M. Bida, Structural performance of precast foamed concrete sandwich panel subjected to axial load, KSCE J. Civil Eng. 22 (4) (2018) 1179–1192.
[82] M. El-Zeadani, R.S. Mr, Y.M. Amran, F. Hejazi, M.S. Jaafar, R. Alyousef, H. Alabduljabbar, Analytical mechanics solution for measuring the deflection of strengthened RC beams using FRP plates, Case Stud. Construct. Mater. 11 (2019), e00272.
[83] A. Siddika, M.H.H. Shojib, M.M. Hossain, M.I. Hossain, M.A. Al Mamun, R. Alyousef, Y.M. Amran, Flexural performance of wire mesh and geotextile-strengthened reinforced concrete beam, SN Appl. Sci. 1 (11) (2019) 1324.
[84] A. Rashad, S. Zeedan, The effect of activator concentration on the residual strength of alkali-activated fly ash pastes subjected to thermal load, Construct. Build. Mater. 25 (7) (2011) 3098–3107.
[85] S.T. Bergold, F. Goetz-Neunhoeffer, J. Neubauer, Quantitative analysis of C–S–H in hydrating alite pastes by in-situ XRD, Cement Concr. Res. 53 (2013) 119–126.
[86] Harry FW. Taylor, Cement Chemistry, Thomas Telford, 1997.